Biogeosciences Discuss., 11, 13029–13065, 2014
www.biogeosciences-discuss.net/11/13029/2014/
doi:10.5194/bgd-11-13029-2014

Biogeosciences Discussions
Open Access

Assessing net community production in a glaciated Alaska fjord

S. C. Reisdorph[1] **and J. T. Mathis**[1,2]

[1]University of Alaska Fairbanks, Ocean Acidification Research Center, 245 O'Neill Bldg., P.O. Box 757220, Fairbanks, AK 99775-7220, 907-474-5995, USA
[2]NOAA – Pacific Marine Environmental Laboratory, 7600 Sandpoint Way NE, Seattle, WA 98115, USA

Received: 6 August 2014 – Accepted: 14 August 2014 – Published: 9 September 2014

Correspondence to: S. C. Reisdorph (screisdorph@alaska.edu)

Published by Copernicus Publications on behalf of the European Geosciences Union.

Abstract

The impact of deglaciation in Glacier Bay (GLBA) has been observed to seasonally impact the biogeochemistry of this marine system. The influence from surrounding glaciers, particularly tidewater glaciers, has the potential to greatly impact the efficiency and structure of the marine food web within GLBA. To assess the magnitude, spatial and temporal variability of net community production (NCP) in a glaciated fjord, we measured dissolved inorganic carbon (DIC), inorganic macronutrients, dissolved oxygen (DO) and particulate organic carbon (POC) between July 2011 and July 2012 in Glacier Bay, AK. Seasonally-averaged data were analyzed on a regional basis to account for distinct biogeochemical differences within the Bay due to spatial variation in rates of primary production and the influence of glacial-fed stratification, particularly in the northern regions. High NCP rates were observed across the Bay ($\sim$ 54 to $\sim$ 81 mmol C m^{-2} d^{-1}) between the summer and fall of 2011. However, between the fall and winter, as well as between the winter and spring of 2012, air–sea fluxes of CO_2 and organic matter respiration made NCP rates negative across most of the Bay as inorganic carbon and macronutrient concentrations returned to pre-bloom levels. The highest carbon production occurred within the lower bay between the summer and fall of 2011 with $\sim 1.3 \times 10^{10}$ g C season^{-1}. Bay-wide, there was carbon production of $\sim 2.6 \times 10^{10}$ g C season^{-1} between the summer and fall. Respiration and air–sea gas exchange were the dominant drivers of carbon biogeochemistry between the fall and winter of 2012. The substantial spatial and temporal variability in our NCP estimates largely reflect glacial influences within the Bay, as melt-water is depleted in macronutrients relative to marine waters entering from the Gulf of Alaska in the middle and lower parts of the Bay. Further glacial retreat will likely lead to additional modifications in the carbon biogeochemistry of GLBA with unknown consequences for the local marine food web, which includes many species of marine mammals.

BGD
11, 13029–13065, 2014

1 Introduction

Glacier Bay (GLBA) lies within the Gulf of Alaska (GOA) coastal ocean and is a pristine glacially influenced fjord that is representative of many other estuarine systems that border the GOA (Fig. 1). GLBA is influenced by freshwater input, primarily from many surrounding alpine and tidewater glaciers. The low-nutrient influx of freshwater into GLBA, which is highest (up to ~ 40 % freshwater in surface waters during the summer; Reisdorph and Mathis, 2014) along the northern regions of the Bay, affects the nutrient loading and, thus, biological production and CO_2 fluxes within the Bay. The southern region of the bay is less affected by this runoff due to distance from the glacial influence and is more influenced by marine waters that exchange through a narrow channel with a shallow entrance sill.

Alaska's coasts contain more than 200 major fjords, though very few have been studied in detail (Etherington et al., 2007). They can be grouped into two distinct regions, a south-central region and a southeast region, each with hydrological differences due to differences in terrestrial and oceanic influences. The south-central fjords, which include Cook Inlet and Prince William Sound (PWS) (Fig. 1), tend to have more open interaction with the oceanic waters of the GOA, while fjords in the southeast, such as GLBA, communicate with the GOA via smaller interconnected channels (Etherington et al., 2007). Glacial influences play an important role in both of these fjord systems, but are more dominant in locations such as GLBA where estuarine-ocean exchange is limited. While PWS and GLBA are highly glacially-influenced and have similar source waters derived from the coastal GOA, PWS is a semi-enclosed fjord that has a relatively direct exchange of waters via Hinchinbrook Entrance and Montague Strait (Musgrave, 2013). Conversely, GLBA has only one entrance over a shallow entrance sill (~ 25 m) (Hooge, 2002) and connects to the GOA through several small channels (Hill et. al., 2009).

Despite GLBA's limited exchange with the open ocean, elevated chlorophyll *a* (chl *a*) concentrations have been observed throughout most of the year, especially from spring through fall (Etherington et. al., 2007) and primary production supports a diverse food

BGD
11, 13029–13065, 2014

web, including endangered species such as humpback whales and Stellar sea lions. Over the past ~ 250 years, GLBA has experienced very rapid deglaciation, which has likely impacted the biological structure of the bay. As the climate continues to warm, additional changes to this ecosystem and marine population have the potential to impact net community production (NCP) within the bay, with cascading effects through the food web, as has been noted in the GOA in regards to decreasing capelin populations (Arimitsu et al., 2008). To better understand the seasonal dynamics of the underlying biogeochemistry in GLBA, we used the seasonal drawdown of the inorganic constituents of photosynthesis within the mixed layer to estimate regional mass flux of carbon and rates of NCP along with air–sea flux rates of CO_2. This approach has been used in other high-latitude regions to assess ecosystem functionality (e.g. Mathis et al., 2009; Cross et al., 2012; Mathis and Questel, 2013).

Previous studies have shown there is wide-ranging variability in rates of primary production within glaciated fjord systems, though NCP data within these ecosystems are sparse. A study by Whitney (2011) looked at nutrient availability and new production in the subarctic Pacific Ocean between 1987 and 2010. He estimated new production between April and September of ~ 7.4 mmol C m^{-2} d^{-1} off of the Canadian coast (48–54° N, 140–128° W) and ~ 5.5 mmol C m^{-2} d^{-1} along the subarctic-subtropical boundary in the north-central Pacific Ocean (36–41° N, 170–150° W). A comprehensive analysis done by Lockwood et al. (2012) combined previous NCP estimates within the Pacific and GOA regions using a ratio of dissolved oxygen to argon for their NCP calculations. Averaging NCP calculations from their study, as well as multiple publications, they estimated daily NCP around Ocean Station Papa (~ 50–55° N, 145° W) of 14 ± 5 mmol C m^{-2} d^{-1}. Additional NCP estimates were done for the northern Pacific region near a chlorophyll front (40–45° N) where rates were 9 ± 5 mmol C m^{-2} d^{-1} and within the Alaska Gyre (~ 50–55° N) where rates were 18 mmol C m^{-2} d^{-1} (Lockwood et al., 2012).

The few NCP studies done in fjord systems similar to that of GLBA have used a variety of instruments and data in their NCP estimations. Using chl *a* data col-

BGD
11, 13029–13065, 2014

lected via a FIRe (Satlantic Instruments) fluorometer, Quigg et al. (2013) found integrated primary productivity within Simpson and Sheep Bays, PWS, varied from ~ 60 to $\sim 90\,\mathrm{mmol\,C\,m^{-2}\,d^{-1}}$. These values are between those estimated by Ziemann et al. (1991) during summer seasons in Auke Bay, AK between 1985 and 1989 ($\sim 8\,\mathrm{mmol\,C\,m^{-2}\,d^{-1}}$) and those from Goering et al. (1973) in and near Port Valdez, AK using ^{14}C (~ 125 to $\sim 333\,\mathrm{mmol\,C\,m^{-2}\,d^{-1}}$).

A study by Aracena et al. (2011) looked at water column productivity in response to surface sediment export production in various Chilean Patagonia fjords (41–56° S). They divided the fjords into four latitudinal regions and calculated primary production rates during the summer between $\sim 35\,\mathrm{mmol\,C\,m^{-2}\,d^{-1}}$ in the more southern regions (52–55° S) and $\sim 488\,\mathrm{C\,m^{-2}\,d^{-1}}$ to the north (41 to ~ 44° S). Fjords within the Central Patagonia region (48–51° S) are strongly influenced by glaciated terrain and freshwater runoff, similar to influences in and around GLBA. In Central Patagonia, Aracena et al. (2011) estimated primary productivity at $\sim 57\,\mathrm{mmol\,C\,m^{-2}\,d^{-1}}$ in the spring, a value comparable to some seasonal estimates in GLBA, and found primary production rates comparable to those of Norwegian fjords (~ 9 to $\sim 360\,\mathrm{mmol\,C\,m^{-2}\,d^{-1}}$).

Few regions of the world still have tidewater glaciers, and Alaskan fjords, such as GLBA, is one such region, along with Greenland, Svalbard, Antarctica, Chile, and the Canadian Arctic (Etherington et al., 2007; Syvitski et al., 1987). Therefore, understanding the dynamics that drive NCP and the associated air–sea CO_2 fluxes within glacially influenced Alaskan fjords can provide insights on how deglaciation may affect carbon budgets in fjords worldwide.

2 Background

Seasonal variation in factors such as light availability and freshwater input, impact physical conditions that are vital to primary production, including stratification, photic depth, and nutrient availability. These drivers of NCP vary temporally and spatially within GLBA. Increasing solar radiation during spring and summer help to set up the strat-

BGD
11, 13029–13065, 2014

ification needed for photosynthetic organisms to remain in the mixed layer and longer daylight hours promote photosynthesis. Low-nutrient glacial runoff is prevalent, and while it aids in stratification, its low macronutrient concentrations dilute available nutrients in the northern regions nearest tidewater outflows. In the lower parts of the Bay, glacial influence is lower and macronutrients are more abundant allowing higher levels of primary production during spring and summer.

GLBA maintains relatively elevated phytoplankton concentrations throughout the year compared to levels observed in similar Alaskan fjords (Hooge, 2002). However, insufficient research has been done on the biological system within GLBA to understand why this occurs. One of the more comprehensive studies (Robards et al., 2003) found zooplankton diversity and abundance to be similar to that throughout the GOA. Within GLBA, areas nearest tidewater glaciers, or recently grounded tidewater inlets, maintained some of the highest prey species (i.e. zooplankton and forage fish) abundances, suggesting the importance of these tidewater-influenced habitats. Forage fish, including capelin, sand lance and walleye Pollock, along with euphausids, were generally found the upper inlets and areas near river and stream outlets. Robard et al. (2003) also found differing fish community structures in the east and west arms, with the east arm primarily supporting capelin with Pollock dominating elsewhere in the bay. In regards to predators (sea birds and marine mammals) in GLBA, Robard et al. (2003) found assemblages to be seasonally dependent, but numerous and diverse. Similar to observations in the GOA and Auke Bay, AK, a peak in zooplankton abundance occurs during late May or early April within lower GLBA. However, unlike the GOA and other estuaries along the GOA, they observed a second, smaller peak in zooplankton abundance in August, though zooplankton densities within the upper regions of the bay generally peak in July (Robard et al., 2003).

During the summer, GLBA is a crucial locale for several marine predators, some of whose populations are declining due to climate change and deglaciation. Spawning and non-spawning adult capelin, a prey species for several marine predators, are more likely to occur in areas nearest tidewater glaciers that have lower temperatures

BGD
11, 13029–13065, 2014

and chl *a* levels coupled with higher turbidity and dissolved oxygen concentrations as compared to other areas of GLBA (Arimitsu et al., 2008). In the GOA, populations of capelin, as well as other favored prey species, have been observed to be declining in association with a reduction of these glacially-influenced habitats and have been linked to reduced populations of higher trophic level predators including harbor seals and red-legged kittiwakes (Arimitsu et al., 2008; Piatt and Anderson, 1996; Trites and Donnelly, 2003). GLBA sustains perhaps one quarter of the worldwide population of breeding Kittlitz's Murrelets (Arimitsu et al., 2008), a seabird classified as critically endangered and proposed for listing under the US Endangered Species Act by the International Union for the Conservation of Nature (IUCN) (Kirchhoff et al., 2013).

Macronutrient concentrations also vary spatially across the bay, partially due to dilution from the low-nutrient glacial influence in the north. These nutrient concentrations are also affected by the metabolic requirements of phytoplankton taken up at average proportions for carbon, nitrogen and phosphate of 106 : 16 : 1 (e.g. Weber, 2010), referred to as the Redfield ratio. Macronutrient uptake within the southern regions closely follows the Redfield ratio. However, the northern regions are highly influenced by low-macronutrient glacial runoff, resulting in nutrient uptake that deviates from the Redfield ratios.

Reisdorph et al. (2014) found dissolved inorganic carbon (DIC) and total alkalinity (TA) concentrations to be lowest within the upper arms of the Bay, while concentrations increased to the south throughout the year, with the largest gradient occurring during summer. However, they found waters across the bay to be well-mixed throughout the water column during winter due to a higher degree of seasonal wind mixing. A similar pattern was observed in the aragonite saturation states (Ω_{Ar}) within the bay with aragonite undersaturation occurring within the upper arms of the bay during though summer. During the fall, Ω_{Ar} were tightly constrained and all surface waters were undersaturated with respect to aragonite.

Aside from primary production, air–sea carbon dioxide (CO_2) flux also impacts carbon concentrations within surface waters. Evans and Mathis (2013) observed instances

BGD
11, 13029–13065, 2014

of both, atmospheric uptake and outgassing, to occur in almost every month in the coastal regions of the GOA, which are the source waters of GLBA. However, uptake of atmospheric CO_2 dominated during the non-winter months, especially in the spring and fall, which coincided with periods of strong winds and undersaturated pCO_2 levels in the surface waters. When annually-averaged, they report that the coastal ocean and continental margin of the GOA act as a strong sink for atmospheric CO_2 with fluxes of −2.5 and −4 mmol CO_2 m^{-2} d^{-1}, but their observations were limited in glacially-influenced waters.

For this paper, we have calculated seasonal NCP and air–sea carbon flux for the four regions within GLBA in order to better understand ecosystem production in a glacially dominated environment, representative of much of the southern coastal AK region.

3 Methods

Ten oceanographic sampling cruises took place between July 2011 and July 2012. Water column samples were collected at six depths (2, 10, 30, 50 100 m and near the bottom) at each station throughout the bay (Fig. 1). Seasonal data was calculated by averaging each measured parameter at each depth for all cruises during the respective seasons. The summer season consists of June, July and August, fall includes September and October; winter is comprised of February and March cruises, and the spring season includes the months of April and May. Data has been averaged regionally within each of the four regions of the Bay (lower bay = LB; central bay = CB; east arm = EA; west arm = WA) (Fig. 1).

Conductivity-temperature-depth (CTD) data were collected on downcasts with a Seabird 19-plus system. Dissolved oxygen (DO) was sampled and processed first to avoid compromising the samples by atmospheric gas exchange. Samples for DO analysis were drawn into individual 115 mL Biological Oxygen Demand (BOD) flasks and rinsed with 4–5 volumes of sample, treated with 1 mL $MnCl_2$ and 1 mL NaI/NaOH, plugged, and the neck filled with DI water to avoid atmospheric exchange. Sam-

BGD
11, 13029–13065, 2014

ples were analyzed within 48 h. Apparent oxygen utilization (AOU) was derived from observed DO concentrations using Ocean Data View calculations in version 4.6.2 (Schlitzer, 2013).

DIC samples were drawn into 250 mL borosilicate bottles. Samples were fixed with a saturated mercuric chloride solution (200 µL), the bottles sealed, and stored until analysis at the Ocean Acidification Research Center (OARC) at the University of Alaska Fairbanks (UAF). High-quality DIC data was attained by using a highly precise (0.02 %; 0.4 µmol kg^{-1}) VINDTA 3C-coulometer system. TA was determined by potentiometric titration with a precision of ~ 1 µmol kg^{-1}. DIC and TA samples were calibrated by routine analysis of seawater certified reference materials (prepared and distributed by Andrew Dickson, UCSD) to ensure accuracy.

Macronutrient samples were filtered through 0.8 µm Nuclepore filters using in-line polycarbonate filter holders into 25 mL HDPE bottles and frozen (−20 °C) until analysis at UAF. Samples were analyzed within several weeks of collection using an Alpkem Rapid Flow Analyzer 300 and following the protocols of Whitledge et al. (1981).

Particulate organic carbon (POC) samples were collected from Niskins into brown 1 L Nalgene bottles and stored for filtering within 2 days of collection. A known volume of samples was filtered through muffled and preweighed 13 mm glass fiber filters using a vacuum pump. Filtered sampled were frozen for transport back to UAF where they were then dried and reweighed. Analyses were completed by OARC at UAF and were run using the methods outlined in Goni et al. (2001).

The partial pressure of CO_2 (pCO_2) was calculated using CO2SYS (version 2.0), a program that employs thermodynamic models of Lewis and Wallace (1995) to calculate marine carbonate system parameters. A standard atmospheric pCO_2 of 395 µatm was used for all seasons. For this study we used K_1 and K_2 constants from Mehrback et al. (1973) and refit by Dickson and Millero (1987), $KHSO_2$ values from Dickson, the seawater pH scale, and $[B]_T$ value from Uppstrom (1974).

BGD
11, 13029–13065, 2014

CO_2 fluxes were calculated using seasonally averaged seawater temperature, wind speed, and seawater and atmospheric pCO_2 data using the equation,

$$\text{Flux} = L \cdot (\Delta pCO_2) \cdot k \quad (1)$$

where L is the solubility of CO_2 at a specified seawater temperature in mmol m^{-3} atm^{-1} and ΔpCO_2 represents the difference between seawater and atmospheric pCO_2 in µatm. k is the steady/short-term wind parameterization in cm h^{-1} at a specified wind speed and follows the equation,

$$k = 0.0283 \cdot U \cdot (Sc/660)^{(1/2)} \quad (2)$$

where U is wind speed in m s^{-1}, Sc is Schmidt number, or the kinematic velocity of the water divided by the molecular diffusivity of a gas in water, and was normalized to 660 cm h^{-1}, equivalent to the Sc for CO_2 in 20 °C seawater (Wanninkhof and McGillis, 1999).

Seawater temperatures for flux calculations were taken from surface bottle CTD data. Wind speeds were obtained from a Bartlett Cove, AK weather station (Station BLTA2) located in GLBA and maintained by the National Weather Service Alaska Region.

NCP calculations were made using the seasonal drawdown of DIC within the mixed layer (upper 30 m) and were normalized to a salinity of 35 to account for the high glacial influence in the northern regions of GLBA. NCP production was calculated for each season between the summer of 2011 and the summer of 2012 according to the equation (Williams, 1993),

$$\text{NCP} = \text{DIC}_{\text{spring}} - \text{DIC}_{\text{summer}} = \Delta\text{DIC}(\text{moles C per unit volume area}) \quad (3)$$

Since this equation only reflects the effects of DIC, this could be accounted for by correction of the seasonal changes in TA (Lee, 2001) using the equation,

$$\Delta\text{DIC}_{\text{Alk}} = 0.5 \cdot (\Delta\text{Alk} + \Delta\text{NO}_3) \quad (4)$$

BGD
11, 13029–13065, 2014

and subtracting this value from the seasonal change in salinity-normalized DIC (nDIC), thus providing an NCP in which the significant process influencing seasonal changes to DIC concentrations is biological productivity (Bates et al., 2005; Mathis et al., 2009; Cross et al., 2012). Air–sea gas exchange can play a lesser role in NCP variation and these are discussed in Sect. 4.5.

Figures 1 through 6 were created using Ocean Data View (ODV) version 4.6.2 (Schlitzer, 2013). Figure 7 was created in Microsoft Excel 2008 version 12.3.6.

4 Results and discussion

4.1 Spatial and seasonal distributions of DIC and nitrate

DIC and nitrate are important inorganic components that are consumed during photosynthesis at various rates throughout the year in GLBA. Figure 2 shows the seasonal relationship between DIC, nitrate and depth between the summer of 2011 and the summer of 2012 with the red line depicting the C : N Redfield Ratio of 106 : 16.

DIC concentrations during the summer of 2011 ranged from ∼ 1400 to 2100 µmol kg^{-1}. DIC variability in the surface waters was a result of primary production and dilution from glacial discharge (Reisdorph and Mathis, 2014), and had a large range (∼ 1400 to 2000 µmol kg^{-1}) with the lowest concentrations in the arms due to the greater influence of tidewater glacier runoff, as well as the upper-CB, where, seasonally, chl *a* concentrations have been observed to be highest (Etherington et al., 2007). Below the surface layer, DIC and nitrate concentrations closely followed the Redfield ratio and were fairly constant throughout the year.

Nitrate concentrations throughout the water column during the summer of 2011 ranged from ∼ 2.5 to ∼ 37 µmol kg^{-1}, with slightly less variability in the surface layer (∼ 2.5 and 24 µmol kg^{-1}). Surface nitrate concentrations were low, but remained > 5 µmol kg^{-1} at all stations, even during times of elevated primary production. Nitrate values were consistently the lowest in the two arms and CB. While there was a large

BGD
11, 13029–13065, 2014

drawdown of nitrate, particularly in spring and summer (as much as 20 µmol kg^{-1} when compared to winter concentrations), surface waters were not depleted at any of the observed stations, indicating that nitrate was being continuously supplied to the surface layer. Additionally, phosphate concentrations (data not shown here) remained above ~ 0.5 µmol kg^{-1}, indicating that it was not the limiting reagent to photosynthesis either. The lowest concentrations of DIC and macronutrients were observed within the arms due to the influence tidewaters glacier runoff, which can likely be attributed to dilution from freshwater runoff, as well as salinity-driven stratification limiting mixing and nutrient replenishment in the mixed layer. Additionally, the unique chemistry of tidewater glacier discharge relative to alpine and stream discharge likely played an important role. Because several glaciers in GLBA are calving directly into the water rather than travel down streambeds that are rich in carbonate and organic sediments, there is little opportunity for the glacial melt to accumulate macronutrients, as is the case with carbonate alkalinity (Reisdorph and Mathis, 2014).

In the fall of 2011, DIC and nitrate concentrations increased in the surface waters as primary production slowed and winds mixing increased. DIC concentrations in these waters ranged from ~ 1700 µmol kg^{-1} to 2040 µmol kg^{-1}, while below the surface DIC concentrations reached ~ 2075 µmol kg^{-1}. Nitrate concentrations during this time were between ~ 12 µmol kg^{-1} and 32 µmol kg^{-1}. Due to decreasing primary production, concentrations were similar within surface waters, ranging from 11 µmol kg^{-1} to 30 µmol kg^{-1}, with the lowest concentrations observed in the arms.

Increased wind mixing and the reduction of glacial input during the winter of 2012 led to full water column mixing, with much more constrained DIC concentrations (~ 1920 µmol kg^{-1} to 2075 µmol kg^{-1}) than during previous seasons and no significant difference between surface concentrations and those at depth. Nitrate concentrations were also similar to those of fall, ranging from ~ 12 µmol kg^{-1} to 33 µmol kg^{-1}. During winter DIC and nitrate concentrations fell near the Redfield ratio, but deviated slightly from Redfield at the highest nitrate concentrations (Fig. 2). This may have been due to nitrification of ammonium by bacteria leading to an increase the nitrate concentra-

BGD
11, 13029–13065, 2014

tion. Another possibility is "carbon overconsumption", the process in which more DIC is taken up than that inferred from the C : N Redfield ratio (Voss et al., 2011). Explanations for carbon overconsumption include the preferential remineralization of organic nitrogen (Thomas and Schneider, 1999) or an increased release of dissolved organic carbon (DOC) (Engel et al., 2002; Schartau et al., 2007).

As temperatures began to warm in the spring of 2012, the onset of glacial melt and primary production reduced DIC and nitrate concentrations in surface waters across the bay. Surface DIC concentrations were between ~ 1750 µmol kg^{-1} and 2025 µmol kg^{-1}, with water column concentrations reaching ~ 2075 µmol kg^{-1} (Fig. 2). Water column nitrate concentrations ranged from ~ 7 µmol kg^{-1} to ~ 31 µmol kg^{-1}, with an observed surface water maximum of ~ 20 µmol kg^{-1}. During the spring DIC and nitrate correlated closely with the Redfield ratio except for two surface samples located at the northernmost ends of each arm (Fig. 2). This deviation may be explained by the fact that these stations were the first to be influenced by glacial runoff during the onset of the glacial melt season.

Further drawdown of DIC and nitrate in surface waters was observed during the summer of 2012 as primary production intensified. Low nutrient glacial runoff was also highest at this time of year, affecting surface water macronutrient concentrations within the arms of the bay (Hooge et al., 2002). However, concentrations did not drop as low as was observed during the previous summer. In 2012 DIC concentrations were between ~ 1545 to 2066 µmol kg^{-1}, while the surface waters had a maximum of ~ 2000 µmol kg^{-1}. Similar to the previous summer, macronutrients did not reach depletion during the summer of 2012, implying they were not the limiting primary productivity, possibly due to nutrient replenishment via tidal pumping. Nitrate concentrations varied from ~ 13 to 33 µmol kg^{-1}, with relatively high surface concentrations between ~ 17 and 31 µmol kg^{-1}. As shown in Fig. 2, the surface nitrate concentration continued to deviate from the Redfield ratio as these macronutrients were increasingly drawn down by primary productivity and diluted by tidewater glacier runoff. The stations most affected were those within the east and west arms, as well as upper CB, where fresh-

BGD
11, 13029–13065, 2014

water influence was greatest. Within the LB, mixing of nutrient-rich marine waters from the GOA likely offset much of the drawdown from primary production and allowed these surface waters to fall closer to the Redfield ratio.

4.2 Rates and masses of NCP

As mentioned in Sect. 3, DIC concentrations in the upper 30 m of the water column, representing the mixed layer depth (MLD), were averaged and normalized to a salinity of 35 in order to estimate rates and masses of NCP between seasons (Fig. 3).

The seasonal transition between the summer and fall of 2011 had the largest rates of NCP observed during the year of study. During this time all NCP rates were positive, signifying enhanced primary productivity in the mixed layer. NCP rates were highest within the east and west arms of the bay at 70.3 ± 3.5 and 81.3 ± 4.1 mmol C m^{-2} d^{-1}, respectively. A similar NCP rate of 68.9 ± 3.4 mmol C m^{-2} d^{-1} was observed in LB, while CB had the lowest rate between of 53.6 ± 2.7 mmol C m^{-2} d^{-1}.

Calculated rates of NCP became negative during the seasonal transitions from fall to winter, as well as from winter to spring. These negative NCP values indicate that air–sea fluxes (discussed in Sect. 4.5) and organic matter respiration were prominent, increasing CO_2 (DIC) concentrations in the surface waters and overwhelming any weaker signal from primary production.

Air–sea flux of CO_2 overwhelmed the biological signal in all regions of GLBA between the fall and winter seasons. Between the fall and winter, the LB experienced the highest degree of CO_2 flux when compared to biological production with a calculated NCP rate of -14.2 ± 0.7 mmol C m^{-2} d^{-1} followed closely by the CB at -11.5 ± 0.6 mmol C m^{-2} d^{-1}. The biological production was overwhelmed by CO_2 influx in the east and west arms (-0.5 ± 0.03 and -1.3 ± 0.1 mmol C m^{-2} d^{-1}), respectively, but to a less degree than in regions to the south.

A similar trend was observed between the winter and spring of 2012 in all regions except for the LB, likely due to its more macronutrient-rich marine influence from the

BGD
11, 13029–13065, 2014

GOA. The CO_2 flux signal exceeded NCP within the east and west arms of the bay, with rates of -36.4 ± 1.8 mmol C m^{-2} d^{-1} and -26.6 ± 1.3 mmol C m^{-2} d^{-1}, respectively, and to a lesser degree in CB with -17.5 ± 0.9 mmol C m^{-2} d^{-1}. The LB was the only region where biological production dominated the CO_2 flux with a positive NCP rate of 17.6 ± 0.9 mmol C m^{-2} d^{-1}, again reflecting the region's nutrient-rich marine influence.

Between the spring and summer of 2012 the primary production signal was evident in the NCP rates. The LB had the highest rate of NCP at 19.4 ± 1.0 mmol C m^{-2} d^{-1}. CB and the EA had similar rates of 17.2 ± 0.9 and 15.7 ± 0.8 mmol C m^{-2} d^{-1}, respectively. The WA displayed a lower rate of NCP at 6.0 ± 0.3 mmol C m^{-2} d^{-1}, possibly the result of the strong low-macronutrient glacial influences along the arm, which may work to hinder production. Additionally, large volumes of glacial flour imparted into the surface waters from runoff during summer may have limited the photic depth and thus impeded some productivity in the upper arms of the bay (Etherington et al., 2007).

The total mass (g C season^{-1}) of carbon produced from NCP was also estimated for each season and are shown in Fig. 4. The largest production of organic carbon occurred between the summer and fall of 2011, with the largest production signal in the LB and decreasing to the north as glacial influence increased. The LB had the largest biomass production of $1.3 \times 10^{10} \pm 6.5 \times 10^{8}$ g C season^{-1}. The CB also had a large amount of production of $5.9 \times 10^{9} \pm 3.0 \times 10^{8}$ g C season^{-1}, followed by the west and east arms with $4.9 \times 10^{9} \pm 2.5 \times 10^{8}$ and $2.0 \times 10^{9} \pm 1.0 \times 10^{9}$ g C season^{-1}, respectively. When summed across the bay we found $\sim 2.6 \times 10^{10} \pm 1.3 \times 10^{9}$ g C season^{-1} produced between the summer and fall of 2011.

As with the rates of NCP during seasonal transitions with low biological activity, the strong influence of air–sea CO_2 flux can be seen in the masses of carbon calculated. Any negative carbon masses indicate a gain in carbon within the surface waters as a result of low biological production and high wind-induced CO_2 flux and community respiration.

Transitioning from fall to winter, there was substantial variability between the marine-dominated LB and the glacially-influenced EA with $-1.7 \times 10^{10} \pm 8.5 \times 10^{8}$ g C season^{-1}

BGD
11, 13029–13065, 2014

and $-9.5 \times 10^7 \pm 4.8 \times 10^6$ g C season^{-1}, respectively. Both regions were dominated by air–sea CO_2 flux. This difference between the northern and southern regions was likely the result of a higher degree of wind and tidal mixing at stations outside of and near the mouth of the bay. Carbon masses calculated from NCP in CB and the WA also indicated lower production and higher air–sea flux, having rates of $-5.0 \times 10^8 \pm 2.5 \times 10^7$ g C season^{-1} and $-8.6 \times 10^9 \pm 4.3 \times 10^8$ g C season^{-1}, respectively. Community respiration and air–sea flux led to a bay-wide total of $\sim -2.6 \times 10^{10} \pm 1.3 \times 10^9$ g C season^{-1}.

The production signal within the arms and central regions of the bay continued to be overwhelmed by air–sea flux between the winter and spring of 2012. In the east and west arms masses were estimated at $-2.2 \times 10^9 \pm 1.1 \times 10^8$ and $-3.3 \times 10^9 \pm 1.7 \times 10^8$ g C season^{-1}, respectively while the CB had a calculated value of $-4.1 \times 10^9 \pm 2.1 \times 10^8$ g C season^{-1}. The LB once again had a positive NCP mass of $6.3 \times 10^9 \pm 3.2 \times 10^8$ g C season^{-1} signifying increased primary production and a decrease in air–sea flux in this region. Across the bay, we estimated a total of $\sim -3.3 \times 10^9 \pm 1.7 \times 10^8$ g C season^{-1} between the winter and spring of 2012.

Between the spring and summer there was increased production across the bay as stratification strengthened and the hours of daylight increased. LB once again had the greatest production with $8.0 \times 10^9 \pm 4.0 \times 10^8$ g C season^{-1}, followed by production within the CB of $4.5 \times 10^9 \pm 2.3 \times 10^8$ g C season^{-1}. During this time of the year the east and west arms exhibited the lowest biomass production, with an NCP in the WA of $8.5 \times 10^8 \pm 4.3 \times 10^7$ g C season^{-1} and $9.2 \times 10^7 \pm 4.6 \times 10^6$ g C season^{-1} in the EA. NCP was likely hindered within the arms by the inundation of low-nutrient glacial runoff that formed a fresh surface layer and imparted glacial flour into the surface waters in these regions. NCP across the entire bay totaled $\sim 1.3 \times 10^{10} \pm 6.5 \times 10^8$ g C season^{-1}.

4.3 Spatial and seasonal distribution of POC

Particulate organic carbon (POC) concentrations were measured at three depths (surface, 50 m, and bottom) for each station and then averaged regionally. Figure 5 shows

BGD
11, 13029–13065, 2014

the regionally averaged POC concentrations and the color bar represents the apparent oxygen utilization (AOU) for each POC samples.

During the summer of 2011 surface water POC concentrations were between ~ 12 and ~ 55 µmol kg^{-1}. Station 20 at the head of the EA had the highest POC concentration at all sampled depths (~ 2 m, ~ 50 m and ~ 160 m). POC concentrations in the surface were ~ 46 µmol kg^{-1} and ~ 42 µmol kg^{-1} at depth, with a local minimum of ~ 30 µmol kg^{-1} at 50 m. The elevated concentrations at this station may have been due to high erosion and sedimentation of recently-grounded Muir glacier. When regionally averaged, the east and west arms had the highest surface POC concentrations of ~ 35 and ~ 33 µmol kg^{-1}, respectively. The WA also exhibited the highest POC concentrations below the surface with ~ 33 µmol kg^{-1} at 50 m and at depth. The arms also exhibited negative AOU of ~ −80 and ~ −64 µmol kg^{-1} in the west and east arms, respectively. The highest positive AOU of ~ 105 µmol kg^{-1} was observed in the bottom waters of the CB. The CB POC concentrations below the surface were similar, at ~ 9 µmol kg^{-1}, while the surface waters had a POC concentration of ~ 28 µmol kg^{-1} indicating relatively high primary production in the surface waters, but little export to depth, perhaps due to reutilization within the surface waters or horizontal advection from tidal action. LB had relatively lower POC concentrations, but were similar at all depth with ~ 15 µmol kg^{-1}. This could have been the result of higher turbulent mixing within the surface waters outside of the bay leading to weaker stratification and increased vertical mixing, as well as resuspension of POC sediment above and around the shallow entrance sill.

POC concentrations decreased rather dramatically, especially within the surface waters as primary production slowed during the fall. A maximum regional POC concentration of ~ 13 µmol kg^{-1} was observed in the surface waters of the WA while surface POC across the other regions were similar, falling between ~ 8 and ~ 9 µmol kg^{-1}. Below the surface layer POC concentrations were low, ranging from ~ 5 to ~ 8 µmol kg^{-1} at both 50 m and at depth. Regionally, all AOU values were positive during the fall of 2011, indicating wide spread organic matter respiration. A maximum regional surface

BGD
11, 13029–13065, 2014

AOU ($\sim 82\,\mu mol\,kg^{-1}$) was estimated for the LB and a minimum ($\sim 2\,\mu mol\,kg^{-1}$) in the surface waters of the CB. During the fall the LB, especially across and seaward of the sill, were well mixed (Reisdorph and Mathis, 2014) and experienced a high degree of air–sea gas exchange (see Sect. 4.5), which likely lowered the oxygen concentration. In this region DIC concentrations were highest ($\sim 2050\,\mu mol\,kg^{-1}$ at all depths) and oxygen saturation was the lowest (not shown) of any region during fall, suggesting turbulent mixing enhanced air–sea flux, taking up DIC and outgassing oxygen.

In the winter of 2012 surface water POC concentrations were not found to exceed $20\,\mu mol\,kg^{-1}$ and AOU across the bay were on the order of $\sim 70\,\mu mol\,kg^{-1}$, suggesting little production was occurring within the bay, but respiration was still present. This is further supported by the negative NCP values described in Sect. 4.2. Surface POC concentrations during the winter ranged from ~ 2 to $\sim 15\,\mu mol\,kg^{-1}$, while POC concentrations at depth were similar, varying between ~ 3 and $16\,\mu mol\,kg^{-1}$. When averaged regionally, the POC maximum in the WA of $\sim 11\,\mu mol\,kg^{-1}$ was observed within the surface waters, while the CB had a subsurface maximum at 50 m of $\sim 5\,\mu mol\,kg^{-1}$. The EA and LB both had maximum POC concentrations in the bottom waters of ~ 14 and $\sim 9\,\mu mol\,kg^{-1}$, respectively. In the LB, where NCP was lowest, the bottom water POC concentration may have been the result of turbulent mixing outside of and across the sill of the bay, which can mix the water column to depth in this region (Reisdorph and Mathis, 2014; Etherington et al., 2007) and likely stir up sediments along the bottom. POC minima throughout the bay occurred at 50 m depth and ranged between ~ 2 and $\sim 9\,\mu mol\,kg^{-1}$, except at stations 24 in LB and station 13 within the CB where POC was at a local maximum at this depth.

POC concentration in the surface waters began to increase during the spring of 2012, primarily within northern regions of the bay. The EA had the greatest increase in surface POC ($\sim 62\,\mu mol\,kg^{-1}$) with concentrations decreasing in the surface water to the south. The WA and CB had similar surface POC concentrations of $\sim 35\,\mu mol\,kg^{-1}$, and $\sim 30\,\mu mol\,kg^{-1}$, respectively. The LB had the lowest surface POC concentrations with $\sim 13\,\mu mol\,kg^{-1}$, while having the highest rate of NCP and AOU ($\sim 93\,\mu mol\,kg^{-1}$).

BGD
11, 13029–13065, 2014

However, the LB subsurface and deep water POC concentrations were the highest of the four regions, ~ 9 µmol kg^{-1} each, and the only region to have a positive AOU in bottom waters, suggesting a larger vertical transport of organic particles out of the surface layer than observed in other regions.

During the summer of 2012, all four regions exhibited regionally averaged POC maxima at the surface. Surface waters across the bay also experienced decreased AOU values and had elevated rates of NCP indicating substantial productivity within these waters. The EA had the highest surface concentration of POC with ~ 50 µmol kg^{-1}, possibly the result of high productivity and strong stratification due to the buoyant glacial melt layer prohibiting particles from sinking out of the surface layer. Below the surface layer, POC concentrations decreased, ranging from ~ 4.5 to ~ 7 µmol kg^{-1} at 50 m and ~ 5 to ~ 8 µmol kg^{-1} at depth. The WA and CB regions had similar surface POC concentrations of ~ 23 µmol kg^{-1}. Surface water across the bay also experienced the lowest AOU values and had high rates of NCP during summer signifying substantial productivity within these waters. The LB exhibited the lowest surface POC concentration with ~ 13 µmol kg^{-1}, while experiencing the highest rate of NCP and AOU concentrations. This was likely the result of more rapid sinking rates of particles out of the surface waters as these waters are more turbulent than the glacially-stratified northern regions of the bay.

4.4 Relationship between DIC and DO

DIC and DO are both indicators of biological production in a marine ecosystem and have a C : O Redfield ratio of 106 : −170 (Anderson et al., 1994). Figure 7 shows the relationship of DIC and DO within Glacier Bay with the Redfield ratio shown by the red line. DIC and DO have an inverse relationship in that DIC is taken up during photosynthesis, while DO is produced, so we'd expect high oxygen saturation states in spring and summer months.

During the summer of 2011, DO concentrations ranged from ~ 190 to ~ 400 µmol kg^{-1}. All samples below the surface layer, as well as surface samples within

BGD
11, 13029–13065, 2014

the LB followed the Redfield ratio, with concentrations at depth between ~ 190 and 280 µmol kg^{-1}. Surface samples of stations within the arms and CB deviated from Redfield, having high DO concentrations and low DIC. Surface DO was higher than that at depth, ranging between ~ 230 and 400 µmol kg^{-1}. The high DO concentrations, coupled with the reduced DIC concentrations in the surface waters indicate enhanced levels of primary production during the summer season. However, in LB, DIC concentrations remained elevated (~ 2030 µmol kg^{-1}) and DO concentrations were low (~ 240 µmol kg^{-1}).

During fall DO concentrations decreased in the surface waters as temperatures cooled and wind mixing reduced stratification, hindering primary production within the surface waters. However, the surface samples within the arms and CB continued to deviate from Redfield. Surface DO concentrations ranged from ~ 210 to ~ 330 µmol kg^{-1} coupled with reduced surface DIC concentrations suggesting primary production was still occurring, albeit at a lesser level than summer. At depth, DO concentrations varied between ~ 200 and 280 µmol kg^{-1} with C : O ratios close to Redfield.

The water column throughout the bay was well mixed during the winter of 2012. All samples, at the surface and at depth, followed Redfield closely with surface waters having slightly higher DO and lower DIC concentrations than those at depth. Surface water DO concentrations were between 250 and ~ 280 µmol kg^{-1}, while deeper waters ranged from ~ 230 to 255 µmol kg^{-1}.

As stratification increased during the spring, production in the surface waters increased. As a result, DIC was drawn down and DO concentrations increased, having a range between ~ 270 and 410 µmol kg^{-1}. DO concentrations were amplified while DIC was reduced at stations in the northern-most regions of both arms. These samples deviated the most from Redfield, while the remaining samples adhered to the Redfield ratio. Below the surface layer, DO concentration throughout the bay ranged from ~ 250 to 280 µmol kg^{-1}.

During the summer of 2012, the surface waters within the two arms and CB continued to diverge from Redfield. DIC concentrations within the more northern regions

BGD
11, 13029–13065, 2014

of the bay (EA, WA, and CB) were increasingly drawn down, while DO concentrations remained high, indicating strengthening productivity in the surface waters. Surface DO concentrations ranged from ∼ 260 to ∼ 410 µmol kg^{-1}, while at depth DO was lower, varying from 200–∼ 270 µmol kg^{-1}.

4.5 Air–sea gas flux

While GLBA itself represents only a small portion of Alaska's coastal environment, the coastal ocean surrounding the GOA has been shown to act as an important sink for atmospheric CO_2 when averaged seasonally, with uptake of 2.5 to 4 mmol C m^{-2} d^{-1} (Evans and Mathis, 2013). Monthly pCO_2 was averaged seasonally and regionally in GLBA to identify the spatial and temporal variability of air–sea CO_2 exchange between the atmosphere and the surface waters of the bay. Figure 7 shows the air–sea fluxes for the four regions of the Bay during each season between the summers of 2011 and 2012, with positive fluxes indicating outgassing of CO_2 and negative fluxes representing uptake of CO_2 from the atmosphere into the surface waters.

During the summer of 2011 regions of oversaturation and undersaturation with respect to the atmospheric CO_2 were observed. Across the bay, winds were relatively low, at ∼ 1.6 m s^{-1}, inhibiting turbulent mixing, allowing for stratification and, thus, primary production. Surface waters of the CB and the WA were undersaturated with respect to atmospheric CO_2 with pCO_2 values of ∼ 250 µatms. The CB has been observed to have abundant chl *a* levels during most of the year (Hooge, 2002) suggesting enhanced primary production that would act to decrease DIC concentrations and pCO_2 in this region. The WA also had diminished DIC concentrations during this summer largely due to the influx of low-macronutrient tidewater runoff. These lower DIC values caused the CB and the WA to act as minor sinks (∼ −0.3 ± 0.02 mmol C m^{-2} d^{-1} each). The LB and EA had much higher seawater pCO_2 values of ∼ 488 µatms and ∼ 463 µatms causing these regions to act as a source for atmospheric CO_2 of ∼ 0.2 ± 0.01 mmol C m^{-2} d^{-1} for each region. In the lower and central regions of the bay surface water temperatures

BGD
11, 13029–13065, 2014

were relatively high at ~ 8.1 °C and 8.5 °C, respectively. Additionally, the LB experiences turbulent mixing due to tidal action across the shallow sill, which can act to inhibit strong stratification and enhance air–sea gas exchange. Within the EA it was likely the influence of low-TA glacial runoff that led to this region's source status. This runoff, low in TA, increased the pCO_2 in the surface waters. During this time of year seawater temperatures were also rising, increasing the pCO_2 of these waters. The combined influence of the reduced TA concentrations and increased temperatures resulted in an oversaturation of CO_2 in the seawater with respect to the atmosphere and overwhelmed any effect from DIC drawdown via primary production.

During the fall of 2011, winds increased slightly to ~ 2.0 m s^{-1} and surface waters in all regions of the Bay were oversaturated with respect to the atmospheric CO_2. The LB experienced the highest pCO_2 at ~ 670 µatms and acted as the largest source for atmospheric CO_2 with a flux of ~ 1.1 ± 0.06 mmol C m^{-2} d^{-1}. The CB also had elevated pCO_2 with ~ 510 µatms leading to outgassing of ~ 0.5 ± 0.03 mmol C m^{-2} d^{-1}. The EA had a pCO_2 value similar to that of the CB (~ 514 µatms) as well as similar CO_2 flux of ~ 0.5 mmol ±0.03 C m^{-2} d^{-1}. Air–sea CO_2 flux in the WA was ~ 0.3 ± 0.02 mmol C m^{-2} d^{-1}, similar to the EA and CB, but had a slightly lower pCO_2 of ~ 482 µatms. The high pCO_2 values observed during fall, despite strong DIC drawdown during summer, may be the result of a variety of interactions. As a result of reduced glacial runoff during fall, TA concentrations increased (Reisdorph and Mathis, 2014). Additionally, surface water temperatures declined allowing them to hold more CO_2 while mixing brought DIC-rich waters from depth to the surface. These processes likely allowed more CO_2 retention in the water, thus increasing pCO_2 and making the bay a source for CO_2 to the atmosphere.

Similar to the fall, surface waters during the winter of 2012 were oversaturated in CO_2 with respect to the atmosphere and all regions experienced outgassing. pCO_2 values were more constrained, especially within the arms and the CB, ranging from ~ 400 µatms in the WA and CB to ~ 432 µatms in the EA. Due to their similar pCO_2 values, as well as similar seawater temperatures (~ 3.5 °C), the WA and CB expe-

BGD
11, 13029–13065, 2014

rienced similar CO_2 fluxes of $\sim 0.03 \pm 0.002$ and 0.06 ± 0.003 mmol C m^{-2} d^{-1}. The EA had a slightly higher surface temperature (~ 4.1 °C) which may have attributed to its higher flux of $\sim 0.18 \pm 0.01$ mmol C m^{-2} d^{-1}. The LB, which experiences the highest degree of turbulent mixing, especially seaward of the sill, had a CO_2 flux of $\sim 0.76 \pm 0.04$ mmol C m^{-2} d^{-1}. Despite winter having the lowest seawater temperatures, wind mixing peaked (~ 2.1 m s^{-1}) and allowed for CO_2-rich waters from depth to enter the surface waters, increasing pCO_2.

In the spring, seawater temperatures increased slightly to ~ 5 °C across the Bay while salinity remained similar to values observed during the winter (~ 29 to 31). However, all regions, except for the LB, transitioned to sinks for atmospheric CO_2. pCO_2 in the LB remained oversaturated with respect to CO_2 at ~ 423 µatms and had a flux of $\sim 0.11 \pm 0.01$ mmol C m^{-2} d^{-1}, likely the result of greater turbulent flow seaward of the sill delaying the formation of strong stratification and inhibiting primary production. Within the other three regions of the bay, surface water temperatures increased slightly, by just over 1 °C, but due to the onset of spring productivity DIC was drawn down in the surface waters, decreasing the pCO_2 and allowing them to become sinks for atmospheric CO_2. The EA had the greatest decrease in pCO_2, dropping from ~ 432 µatms to ~ 167 µatms and exhibiting seasonal outgassing of $\sim -0.87 \pm 0.04$ mmol C m^{-2} d^{-1} between the winter and spring. The WA and CB regions acted in a similar manner. The reduction in pCO_2 within these two regions was also the result of increased primary production drawing down DIC in the surface waters causing them to become a seasonal sink for CO_2, taking up $\sim -0.39 \pm 0.02$ mmol C m^{-2} d^{-1} in the CB and $\sim -0.60 \pm 0.03$ mmol C m^{-2} d^{-1} in the glacially-influenced WA.

During the summer of 2012 CO_2 over- and undersaturation of surface waters varied regionally, with surface waters in the northern regions becoming increasingly saturated with respect to atmospheric CO_2. While pCO_2 in the EA did increase from the spring, it was still less than atmospheric at ~ 337 µatms causing $\sim -0.13 \pm 0.01$ mmol C m^{-2} d^{-1} of ingassing. The increase in pCO_2 may have been due to a small increase in seawater temperature of ~ 1 °C coupled with a reduction in TA (Reisdorph and Mathis,

BGD
11, 13029–13065, 2014

2014) overwhelming the drawdown in DIC from primary production. The CB was a stronger sink for CO_2 with a lower pCO_2 of ~200 µatms and a flux of ~ −0.44 ± 0.02 mmol C m^{-2} d^{-1}. This reduction in pCO_2 was likely due to high levels of primary production in this region as it has been noted to have some of the highest chl *a* levels, as well as high nutrient replenishment from tidal mixing between the mixed waters of LB and the stratified waters within the CB (Hooge, 2002). The remaining regions, the LB and WA, acted as sources for atmospheric CO_2 during this summer with pCO_2 values of ~ 411 µatms and ~ 507 µatms, respectively. The LB experiences the highest degree of turbulent or tidal mixing across the sill, as well as seaward of the sill, inhibiting stratification and primary production and causing it act as a source for atmospheric CO_2 year-round. During the summer of 2012, the LB experienced a near-neutral flux of ~ 0.04 ± 0.002 mmol C m^{-2} d^{-1}. The WA was also oversaturated with respect to atmospheric CO_2 with a pCO_2 of ~ 507 µatms and a flux of ~ 0.26 ± 0.01 mmol C m^{-2} d^{-1}. The difference between the sink/source status of the east and west arms of the bay was likely the result of differences in glacial influences. The WA is much more influenced by low-TA glacial runoff as it has the majority of the tidewater glaciers along its length. During the summer of 2012, these glaciers caused a higher degree of TA dilution than was observed within the WA, a difference of ~ 100 µmol kg^{-1}. The upper end of WA also had the lowest DIC concentrations observed during this summer also likely due to the high tidewater glacier runoff, which tends to be low in macronutrients.

5 Conclusions

GLBA experiences a high degree of spatial and temporal variability in biogeochemical characteristics throughout the year. Environmental influences vary seasonally along a gradient from the glacially-influenced northern regions within the arms to the marine-influenced LB. This imparts spatial differences in stratification and macronutrient availability that effect biological processes and thus, rates of NCP.

BGD
11, 13029–13065, 2014

We have calculated regional NCP values for each seasonal transition from the summer of 2011 through summer 2012 for GLBA. Despite GLBA's limited exchange with the marine waters of the GOA, it has been observed to have elevated primary production through most of the year (Hooge, 2002), perhaps due to tidal pumping, and has a marine predator presence in all seasons. However, rapid deglaciation within GLBA over the past ~ 250 years has imparted a high volume of fresh glacial runoff, a portion of which has been from tidewater glaciers that melt directly into the bay, affecting stratification, macronutrient concentrations and influencing air–sea CO_2 exchange.

Between the summers of 2011 and 2012, nutrient concentrations in GLBA tended to be lowest in the surface waters of the arms, though never reaching depletion, during the summer season when glacial runoff, primary production (Fig. 2), and DO concentrations (Fig. 6) were highest. Rates of NCP were highest during the transition between summer and fall of 2011, with regional NCP rates ranging from ~ 54 to ~ 80 mmol C m^{-2} d^{-1}. Rates during the summer of 2012 were lower, between ~ 6 and ~ 20 mmol C m^{-2} d^{-1}.

Between the fall of 2011 and winter of 2012, as well as between the winter and spring of 2012, air–sea gas exchange overwhelmed any production signal across the bay. The one exception was LB between winter and spring where NCP rates were positive, likely due to earlier replenishment of nutrients from marine source waters. Although air–sea flux overwhelmed NCP seasonally, fluxes were minimal, with maximum outgassing of ~ 1.1 mmol C m^{-2} d^{-1} occurring in LB during the fall of 2011. While the direction of fluxes varied seasonally and regionally, LB acted as a small source for atmospheric CO_2 during all seasons of the study. During the summer of 2012 areas of CO_2 over- and undersaturation varied, with the LB and WA acting as sources for atmospheric CO_2 and the CB and EA acting as sinks. NCP followed this pattern with a maximum in the LB of 8.0×10^9 g C season^{-1}, followed by the CB with 8.5×10^8 g C season^{-1}. NCP was lowest within the WA (9.2×10^7 g C season^{-1}), likely due to low-TA, low-macronutrient tidewater glacier runoff slowing primary production. Despite a sustained level of primary production in the WA, pCO_2 in this region remained oversaturated (~ 506 µatm)

BGD
11, 13029–13065, 2014

with respect to the atmosphere. This was attributed to the low-TA glacial runoff diluting TA concentrations in the surface water leading to elevated pCO_2. This, coupled with the fact that these warmer summer waters have inherently higher pCO_2, caused pCO_2 levels to remain elevated despite sustained biological production. It is clear from our observations that highly glaciated systems like GLBA behave much differently than open ocean regions, as well as glaciated systems with less restricted marine exchange like PWS, when it comes to CO_2 fluxes. The complex interactions between NCP, temperature and TA cause GLBA to behave much differently than the adjacent GOA, which has been shown to be a significant sink for atmospheric CO_2 (Evans and Mathis 2014).

The impact of rapid deglaciation in GLBA can be observed in the seasonal impacts on the biogeochemistry of this marine system. The influence of surrounding glaciers, especially tidewater glaciers, has the potential to significantly impact the efficiency and makeup of the marine food web within GLBA. Some prey species, such as capelin, thrive nearest the tidewater glaciers, most of which are currently receding and thinning, leaving these species with a smaller, less optimal habitat and affecting predators within higher tropic levels. A similar occurrence in the GOA saw a decline in predator species, such as harbor seals and red-legged kittiwakes, as the result of glacial recession (Aritmisu, 2008). The full impact that deglaciation has on a marine system like GLBA, and the numerous similar systems along the Alaskan GOA coast, is currently unknown. However, the coastal margin of the GOA has been estimated at ~ 3000 km, or ~ 1.5 times the length of the US continental margin between northern Washington and southern California and, therefore needs more study and should be considered an area of vital importance to the regional carbon budget.

Acknowledgements. Thanks to the National Park Service for supporting this work through grant number G7224 to the University of Alaska Fairbanks. We would also like to thank Lewis Sharman and NPS staff members in Gustavus and Juneau, AK for their help in sample collection, logistics and editing. We also want to thank the staff and visitors of Glacier Bay National Park and Preserve, as well as the community of Gustavus for their support and interest in this project.

BGD
11, 13029–13065, 2014

References

Anderson, L. A. and Sarmiento, J. L.: Redfield ratios of remineralization determined by nutrient data analysis, Global Biogeochem. Cy., 8, 65–80, 1994.

Aracena, C., Lange, C. B., Luis Iriarte, J., Rebolledo, L., and Pantoja, S.: Latitudinal patterns of export production recorded in surface sediments of the Chilean Patagonian fjords (41–55° S) as a response to water column productivity, Cont. Shelf Res., 31, 340–355, doi:10.1016/j.csr.2010.08.008, 2011.

Arimitsu, M. L., Piatt, J. F., Litzow, M. A., Abookire, A. A., Romano, M. D., and Robards, M. D.: Distribution and spawning dynamics of capelin (Mallotus villosus) in Glacier Bay, Alaska: a cold water refugium, Fish. Oceanogr., 17, 137–146, doi:10.1111/j.1365-2419.2012.00616.x, 2008.

Bates, N. R., Best, M. H. P., and Hansell, D. A.: Spatio-temporal distribution of dissolved inorganic carbon and net community production in the Chukchi and Beaufort Seas, Deep-Sea Res. Pt. II, 52, 3303–3323, doi:10.1016/j.dsr2.2005.10.005, 2005.

Cross, J. N., Mathis, J. T., and Bates, N. R.: Hydrographic controls on net community production and total organic carbon distributions in the eastern Bering Sea. Deep-Sea Res. Pt. II, 65–70, 98–109, doi:10.1016/j.dsr2.2012.02.003, 2012.

Engel, A., Goldthwait, S., Passow, U., and Alldredge, A.: Temporal decoupling of carbon and nitrogen dynamics in a mesocosm diatom bloom, Limnol. Oceanogr., 47, 753–761, doi:10.4319/lo.2002.47.3.0753, 2002.

Etherington, L., Hooge, P. N., Hooge, E. R., and Hill, D. F.: Oceanography of Glacier Bay, Alaska?: implications for Biological Patterns in a Glacial Fjord Estuary, Estuar. Coast., 30, 927–944, 2007.

Evans, W. and Mathis, J. T.: The Gulf of Alaska coastal ocean as an atmospheric CO_2 sink, Cont. Shelf Res., 65, 52–63, doi:10.1016/j.csr.2013.06.013, 2013.

Gelatt, T. S., Trites, A. W., Hastings, K., Jemison, L., Pitcher, K., and O'Corry-Crow, G.: Population trends, diet, genetics, and observations of Steller sea lions in Glacier Bay National Park, in: Proceedings of the Fourth Glacier Bay Science Symposium, edited by: Piatt, J. F. and Gende, S. M., 26–28 October 2004, US Geological Survey Scientific Investigations Report, 2007–5047, 145–149, 2007.

BGD
11, 13029–13065, 2014

Goering, J. J., Patton, C. J., and Shiels, W. E.: Primary production, in: Environmental Studies of Port Valdez, edited by: Hood, D. W., Shiels, W. E., and Kelley, E. J., Institute of Marine Science Occasional Publications No. 3, University of Alaska, Fairbanks, AK, 253–279, 1973.

Goñi, M. A., Teixeira, M. J., and Perkey, D. W.: Sources and distribution of organic matter in a river-dominated estuary (Winyah Bay, SC, USA), Estuar. Coast. Shelf S., 57, 1023–1048, doi:10.1016/S0272-7714(03)00008-8, 2003.

Helmuth, T. and Schneider, B.: The seasonal cycle of carbon dioxide in Baltic Sea surface waters, J. Marine Syst., 22, 53–67, 1999.

Hill, S. J. Ciavola, L. Etherington, M. J. and Klaar, D. F.: Estimation of freshwater runoff into Glacier Bay, Alaska and incorporation into a tidal circulation model, Estuar. Coast. Shelf S., 82, 95–107, 2009.

Hooge Elizabeth Ross Hooge, P. N.: Fjord oceanographic processes in Glacier Bay, Alaska, Glacier Bay Report, Gustavus, AK, 2002.

Kirchhoff, M. D., Lindell, J. R., and Hodges, J. I.: From critically endangered to least concern? – a revised population trend for the Kittlitz's Murrelet in Glacier Bay, Alaska, Condor 116, 24–34, doi:10.1650/CONDOR-13-123.1, 2014.

Lee, K.: Global net community production estimated from the annual cycle of surface water total dissolved inorganic carbon, Limnol. Oceanogr., 46, 1287–1297, doi:10.4319/lo.2001.46.6.1287, 2001.

Mathis, J. T. and Questel, J. M.:. The impacts of primary production and respiration on the marine carbonate system in the western Arctic: implications for CO_2 fluxes and ocean acidification, Cont. Shelf Res., 67, 42–51, doi:10.1016/j.csr.2013.04.041, 2013.

Mathis, J. T., Bates, N. R., Hansell, D. A., and Babila, T.: Net community production in the northeastern Chukchi Sea, Deep-Sea Res. Pt. II, 56, 1213–1222, doi:10.1016/j.dsr2.2008.10.017, 2009.

Piatt, J. F. and Anderson, P.: Response of common murres to the Exxon Valdez oil spill and long-term changes in the Gulf of Alaska marine ecosystem, Am. Fish. Soc. Symp., 18, 720–737, 1996.

Quigg, A., Nunnally, C., McInnes, A., Gay, S., Rowe, G., Dellapenna, T., and Davis, R.: Hydrographic and biological controls in two subarctic fjords: an environmental case study of how climate change could impact phytoplankton communities, Mar. Ecol.-Prog. Ser., 480, 21–37, doi:10.3354/meps10225, 2013.

BGD
11, 13029–13065, 2014

Reisdorph, S. C. and Mathis, J. T.: The dynamic controls on carbonate mineral saturation states and ocean acidification in a glacially dominated estuary, Estuar. Coast. Shelf S., 144, 8–18, 2014.
Renner, M., Arimitsu, M. L., and Piatt, J. F.: Structure of marine predator and prey communities along environmental gradients in a glaciated fjord, Can. J. Fish. Aquat. Sci., 69, 2029–2045, doi:10.1139/f2012-117, 2012.
Robards, M., Drew, G., Piatt, J., Anson, J. M., Abookire, A., Bodkin, J., Hooge, P., and Speckman, S.: Ecology of Selected Marine Communities in Glacier Bay? Zooplankton, Forage Fish, Seabirds and Marine Mammals, Anchorage, AK, Gustavus, AK, 1–156, 2003.
Schartau, M., Engel, A., Schröter, J., Thoms, S., Völker, C., and Wolf-Gladrow, D.: Modelling carbon overconsumption and the formation of extracellular particulate organic carbon, Biogeosciences, 4, 433–454, doi:10.5194/bg-4-433-2007, 2007.
Schlitzer, R.: Ocean Data View, available at: http://odv.awi.de, 2013.
Syvitski, J. P. M., Burrell, D. C., and Skei, J. M.: Fjords: Processes and Products, Springer-Verlag Inc, New York, 1987.
Trites, A. W. and Donnelly, C. P.: The decline of Steller sea lions Eumetopias jubatus in Alaska?, Mamm. Rev., 33, 3–28, 2003.
Voss, M., Baker, A., Bange, H. W., Conley, D., Cornell, S., Deutsch, B., Engel, A., Ganeshram, R., Garnier, J., Heiskanen, A. S., Jickells, T., Lancelot, C., Mcquatters-Gollop, A., Middelburg, J., Schiedek, D., Slomp, C. P., and Conley, D. P.: Nitrogen processes in coastal and marine ecosystems, in: The European Nitrogen Assessment, edited by: Sutton, M. A., Howard, C. M., Erisman, J. W., Billen, G., Bleeker, A., Grennfelt, P., van Grinsven, H., and Grizzetti, B., Cambridge University Press, New York, 147–176, 2011.
Wanninkhof, R. and McGillis, W. R.: A cubic relationship between air–sea CO_2 exchange and wind speed, Geophys. Res. Lett., 26, 1889–1892, 1999.
Weber, T. S. and Deutsch, C.: Ocean nutrient ratios governed by plankton biogeography, Nature, 467, 550–554, doi:10.1038/nature09403, 2010.
Whitledge, T. E., Malloy, S. C., Patton, C. J., and Wirick, C. D.: Automated Nutrient Analyses in Seawater, Upton, New York, 1981.
Whitney, F. A.: Nutrient variability in the mixed layer of the subarctic Pacific Ocean, 1987–2010, J. Oceanogr., 67, 481–492, doi:10.1007/s10872-011-0051-2, 2011.

BGD
11, 13029–13065, 2014

Williams, P. J.: On the definition of plankton production terms, in: Measurements of Primary Production from the Molecular to the Global Scale, edited by: Li, W. K. W. and Maestrini, S. Y., ICES Mar. Sci. Symp., 197, 9–19, 1993.

Ziemann, D. A., Conquest, L. D., Olaizola, M., and Bienfang, P. K.: Interannual variability in the spring phytoplankton bloom in Auke Bay, Alaska, Mar. Biol., 109, 321–334, 1991.

BGD

11, 13029–13065, 2014

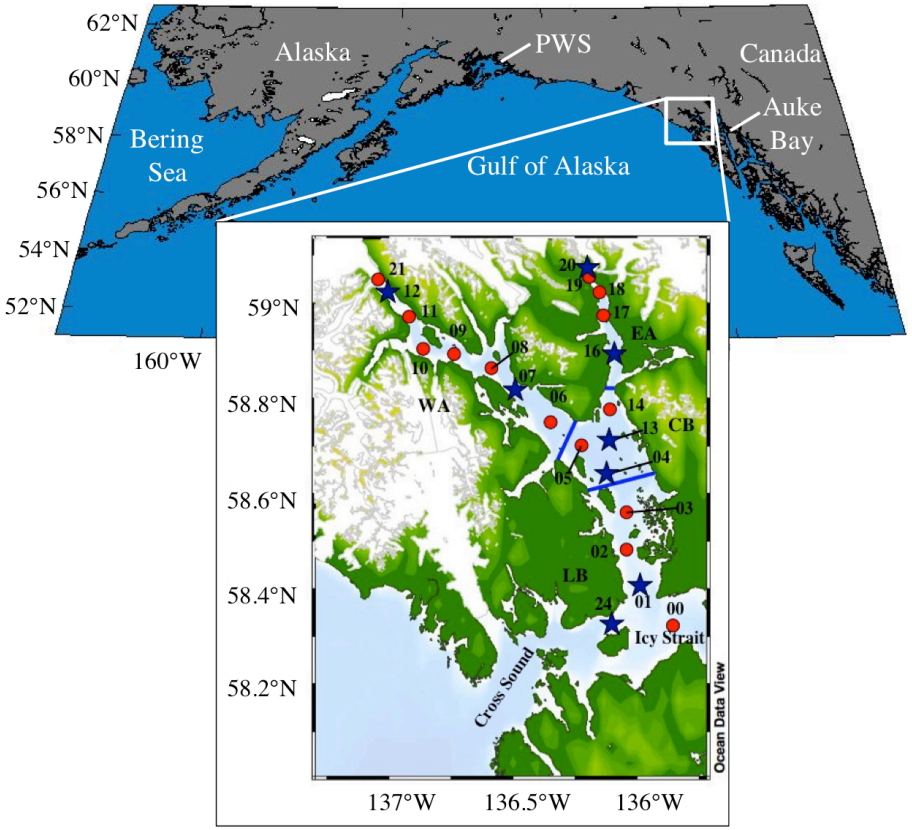

Figure 1. Glacier Bay location and oceanographic sampling station map – blue lines denote regional boundaries. Red dots show all oceanographic station locations with station number. Purple stars represent "core" station location. LB = lower bay, CB = central bay, EA = east arm, WA = west arm.

BGD
11, 13029–13065, 2014

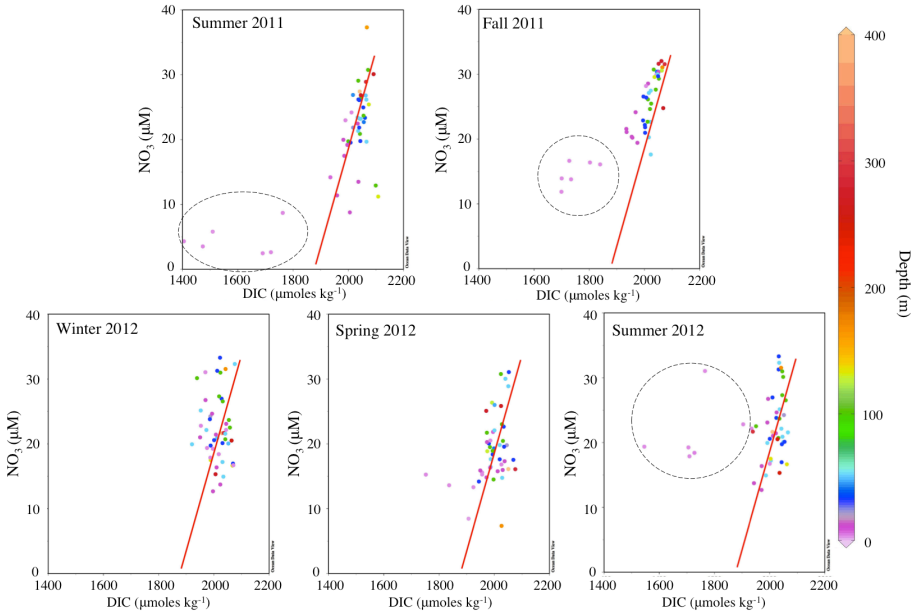

Figure 2. Seasonal DIC vs. NO_3 vs. depth – scatter plots of DIC concentrations vs. NO_3 concentrations for each season between the summer of 2011 and the summer of 2012. Color bar represents depth in m. The red line depicts the C : N Redfield ratio of 106 : 16. Dotted circles highlight samples that deviate from Redfield.

BGD
11, 13029–13065, 2014

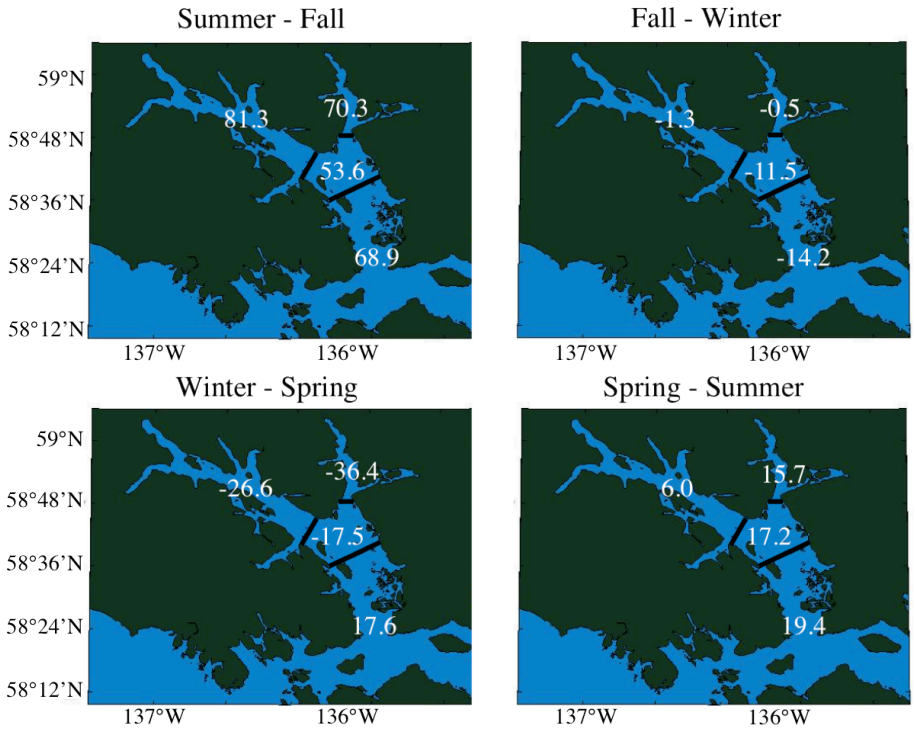

Figure 3. Regional rates of NCP – regional rates of NCP in mmol C m^{-2} d^{-1} for seasonal transitions from summer to fall of 2011 in the upper left through the spring to summer of 2012 in the lower right.

BGD
11, 13029–13065, 2014

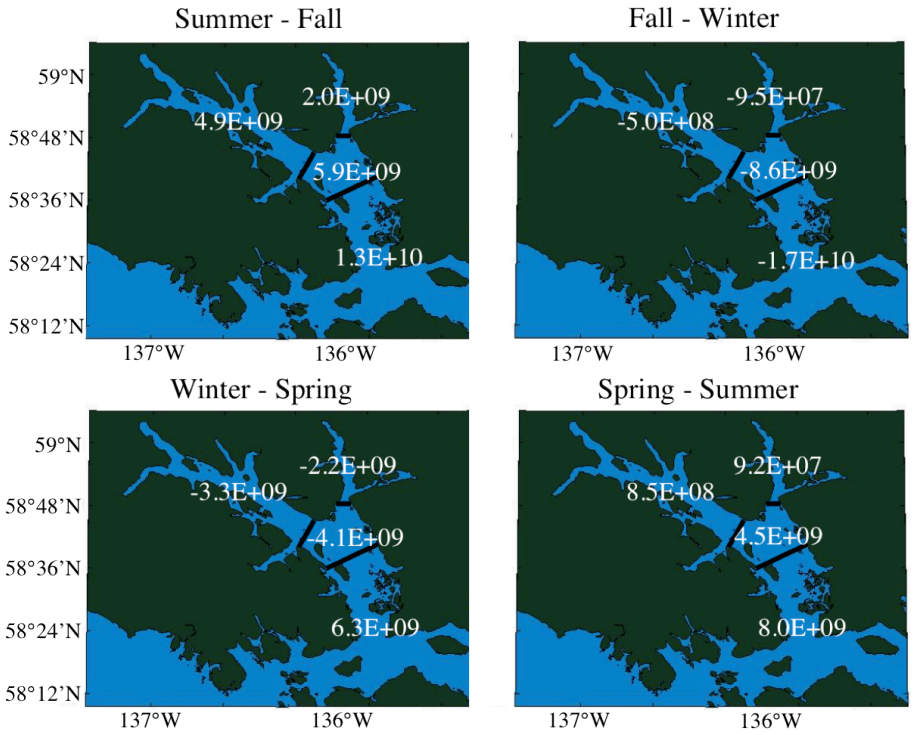

Figure 4. Regional masses of NCP – regional masses of NCP in g C season^{-1} for seasonal transitions from summer to fall of 2011 in the upper left through the spring to summer of 2012 in the lower right.

BGD
11, 13029–13065, 2014

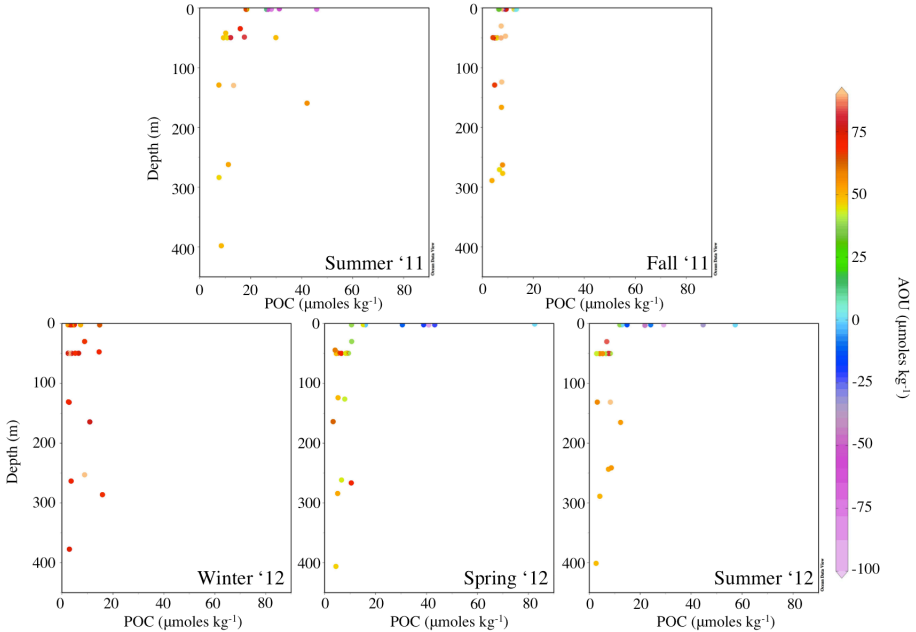

Figure 5. Seasonal POC vs. depth vs. AOU – seasonal scatter plots of POC concentrations vs. depth for each season between the summer of 2011 through the summer of 2012. Color bar represents AOU in $\mu mol\,kg^{-1}$.

BGD
11, 13029–13065, 2014

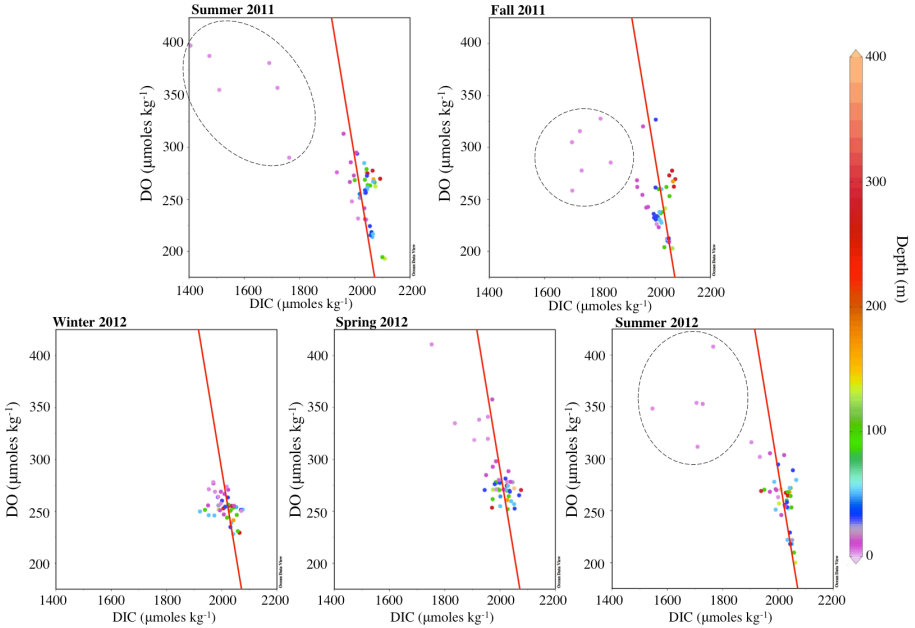

Figure 6. Seasonal DIC vs. DO vs. depth – scatter plots of DIC concentrations vs. DO concentrations for each season between the summer of 2011 and the summer of 2012. Color bar represents depth in m. The red line depicts the C : O Redfield ratio of 106 : −170. Dotted circles highlight samples that deviate from Redfield.

BGD
11, 13029–13065, 2014

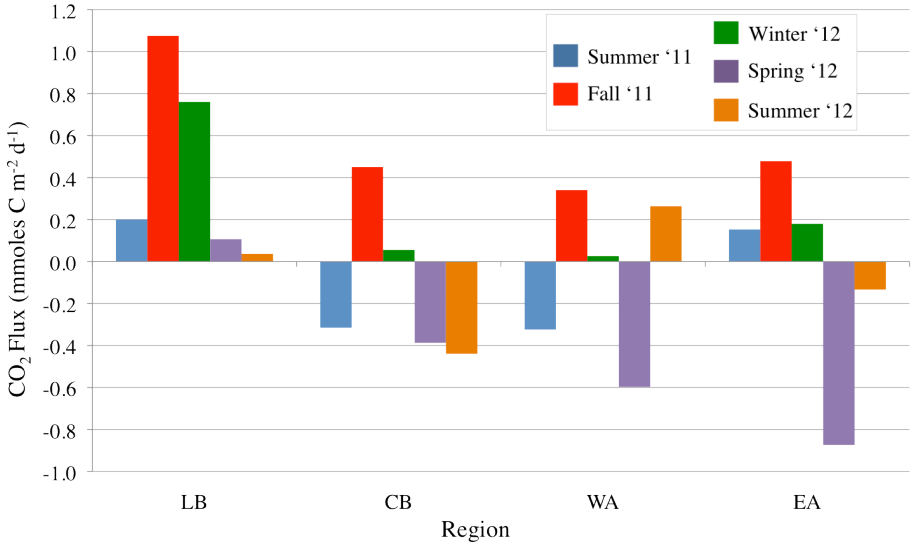

Figure 7. Air–sea CO_2 flux – seasonal air–sea CO_2 fluxes by region in mmol C m^{-2} d^{-1}. Blue represents the summer of 2011, red = fall of 2011, green = winter of 2012, purple = spring of 2012, yellow = summer of 2012.

BGD
11, 13029–13065, 2014